12-1-2005

Telling the truth from lie in individual subjects with fast event-related fMRI

Daniel D. Langleben
University of Pennsylvania, langlebe@upenn.edu

James Loughead
University of Pennsylvania

Warren B. Bilker
University of Pennsylvania, wbilker@cceb.upenn.edu

Kosha Ruparel
University of Pennsylvania, ruparel@bbl.med.upenn.edu

Anna Rose Childress
University of Pennsylvania, childress_a@mail.trc.upenn.edu

See next page for additional authors

Telling the truth from lie in individual subjects with fast event-related fMRI

Abstract

Deception is a clinically important behavior with poorly understood neurobiological correlates. Published functional MRI (fMRI) data on the brain activity during deception indicates that, on a multisubject group level, lie is distinguished from truth by increased prefrontal and parietal activity. These findings are theoretically important; however, their applied value will be determined by the accuracy of the discrimination between single deceptive and truthful responses in individual subjects. This study presents the first quantitative estimate of the accuracy of fMRI in conjunction with a formal forced-choice paradigm in detecting deception in individual subjects. We used a paradigm balancing the salience of the target cues to elicit deceptive and truthful responses and determined the accuracy of this model in the classification of single lie and truth events. The relative salience of the task cues affected the net activation associated with lie in the superior medial and inferolateral prefrontal cortices. Lie was discriminated from truth on a single-event level with an accuracy of 78%, while the predictive ability expressed as the area under the curve (AUC) of the receiver operator characteristic curve (ROC) was 85%. Our findings confirm that fMRI, in conjunction with a carefully controlled query procedure, could be used to detect deception in individual subjects. Salience of the task cues is a potential confounding factor in the fMRI pattern attributed to deception in forced choice deception paradigms.

Author(s)

Daniel D. Langleben, James Loughead, Warren B. Bilker, Kosha Ruparel, Anna Rose Childress, Samantha I. Busch, and Ruben Gur

Telling truth from lie in individual subjects with fast event-related fMRI

Daniel D. Langleben [*], James W. Loughead, Warren B. Bilker, Kosha Ruparel, Anna Rose Childress, Samantha I. Busch, Ruben C. Gur

INTRODUCTION

Recent changes in the defense priorities of the industrialized nations have increased an already strong demand for an objective means of detecting concealed information. The brain correlates of deception are not well understood, though it is a complex behavior that is likely to engage theory of mind, recall, response inhibition, and working memory. In addition to the forensic applications, understanding the neurobiology of deception could provide an important link between psychodynamic and biological psychology [Spence et al., [2004]]. Elucidaiton of the functional anatomy with valid models of deception, followed by a careful assessment of the accuracy of each specific model in discerning truth from lie, is a prerequisite for the successful translation of research findings into a clinically useful method of identification of deceptive behavior [Wolpe et al., [2005]]. Deception can be defined simply as "denying what is" [Augustine, [1948]]. Contemporary definitions emphasize an intentional effort to instill a false belief [Gur and Sackeim, [1979]] in an unknowing target [Ekman, [2001]; Vrij, [2001]].

Currently, "polygraph" is the principal physiological method of lie-detection [Stern, 2004]. Its specificity is limited because it relies on the correlates of peripheral nervous system activity, while deception is a cognition event with top-down control by the central nervous system (CNS). Experiments using CNS measures obtained by electroencephalography (EEG) or functional magnetic resonance imaging (fMRI) provide hope for more accurate detection of deception by comparing the time course and topography of regional brain activity during exposure to cues designed to elicit truth and lie [Rosenfeld et al., [1988]; Spence et al., [2004]].

Several fMRI studies reported increased prefrontal and parietal activity during lie, with a subset reporting anterior cingulate cortex (ACC) activation or prolonged response time (RT) with lie [Ganis et al., [2003]; Kozel et al., [2004]; Langleben et al., [2002]; Lee et al., [2002]; Nunez et al., [2005]; Spence et al., [2001]]. Based on these findings, deception has been conceptualized as inhibition of truth and generation of lie mediated by the prefrontal cortex, with truth being a "routine" response mediated by the posterior structures [Langleben et al., [2002]; Spence et al., [2004]].

Critical questions remain concerning the use of fMRI in lie detection. First, the pattern of activation reported in deception studies was also observed in studies of working memory, error monitoring, response selection, and "target" detection [Hester et al., [2004]; Huettel and McCarthy, [2004]; Zarahn et al., 2004]. Second, inference in the General Linear Model (GLM) analysis of blood oxygenation level-dependent (BOLD) fMRI is based on a contrast of conditions, making the choice of a control condition critical. Thus, the difference in the attentional value (salience) of the cue (condition) intended to elicit "lie" and the control "truth" may have confounded previous studies [Cabeza et al., [2003]; Gur et al., [2004]; Langleben et al., [2002]]. Finally, the sensitivity and specificity with which an fMRI experiment can discriminate lie from truth in the individual subject or single event level is unknown. Our hypotheses were:

1 The magnitude and topography of the differences between lie and truth is affected by the relative salience of the target and control items:

a Lie contrasted with truth condition of lower salience will yield a pattern of activation seen in target detection and deception tasks including the inferior lateral prefrontal (Brodmann area (BA) 44-47), dorsolateral and medial superior and middle frontal gyri (BA 6, 8-10), the anterior cingulate cortex (BA 24/32), and the superior and inferior parietal lobule (BA 7, 40);

b Lie contrasted with truth condition of equal or higher salience will result in activation in a subset of the regions, activated in the nonsalience-controlled contrast, predominantly associated with response inhibition and selection (e.g., the inferior lateral prefrontal gyri).

2 In individuals, single lie and truth events can be discriminated with reasonable and quantifiable accuracy.

SUBJECTS AND METHODS

Participants

Twenty-six right-handed male undergraduate students (mean age = 19.36, standard deviation (SD) = 0.5). After a complete description of the study, written informed consent was obtained.

Task

We used a modification (GKT2) of the previously reported Guilty Knowledge Task (GKT2) [Langleben et al., [2002]]. A pseudorandom sequence of photographed playing cards was presented. The series included five stimulus classes: (1) Lie (5 of clubs or 7 of spades); (2) Truth (5 of clubs or 7 of spades); (3) recurrent distracter (2 of hearts); (4) variant distracter (remaining cards 2-10, all suits); and (5) null (back of a card). To match the attentional demands, the assignment of lie and truth card occurred at the instruction session (see below). Cards were presented for 2 s followed by a variable ISI (0-16 s) during which the null condition (192 total) was displayed. Twenty-four Lie, Truth, and recurrent distracter cards and 168 variant distracter cards were shown. Participants were instructed to press a left button (yes) to confirm that a card was in their possession or the right button (no) to deny it. A total of 432 stimuli were presented with a total session length of 14.4 min.

Stimuli were rear-projected to the center of the visual field using a video projector (PowerLite 7300; Epson America, Long Beach, CA) viewed through a head coil-mounted mirror. Stimuli presentation was synchronized with image acquisition using the PowerLaboratory platform [Chute and Westall, [1997]]. Responses were made by button press on a fiberoptic-response keypad (fORP; Current Design, Philadelphia, PA). Participants were randomly assigned use of their dominant or nondominant hand and responses were recorded via a fORP.

Instruction Protocol

Participants were presented an envelope containing two cards (5 of clubs and 7 of spades) and $20. The principle investigator (D.D.L.) instructed participants to deny possession of one of the cards and acknowledge possession of the other in the imaging phase of the study. Participants were told they could keep the $20 only if successful in concealing the identity of the lie card during the scan session. Participants were escorted to the scanner by a third party and instructed by the fMRI investigator (J.W.L.) to respond to each trial as accurately and truthfully as possible. After the session, participants were debriefed, informed that the compensation was not contingent on performance, queried about the lie card, and asked if they employed any strategy during the task.

Image Acquisition

Images were acquired with blood-oxygen level dependent (BOLD) imaging [Bandettini et al., [1992]] on a clinical 3 T Siemens Trio Scanner (Iselin, NJ). A 5-min, magnetization-prepared, rapid-acquisition gradient echo image (MPRAGE) was acquired for anatomic overlays of functional data and spatial normalization [Talairach and Tournoux, [1988]]. BOLD imaging used a 33-slice whole-brain, single-shot gradient-echo (GE) echo-planar (EPI) sequence (TR/TE = 2000/21 ms, FOV = 240 mm, matrix = 64 × 64, slice thickness/gap = 4/0 mm). This sequence delivered a nominal voxel resolution of 3.75 × 3.75 × 4 mm.

Data Analysis

Percent correct and median reaction time (RT; in milliseconds) were calculated for each stimulus class (Table 1). Differences in percent correct and reaction time among the four classes were evaluated using separate repeated measures analysis of variance (ANOVA). To satisfy the normality assumptions of ANOVA, the arcsine transformation [Cohen, [1988]] was applied to the percentages.

Table I. Percent correct and response time for all stimuli classes

	Percent correct	Response time (ms)
Varied distracter	96 (0.79)	634 (17)
Repeat distracter	98 (0.26)	654 (20)

Lie	97 (0.94)	717 (24)
Truth	93 (1.25)	806 (27)

fMRI data were preprocessed and analyzed with SPM2 (Wellcome Department of Cognitive Neurology, London, UK). Images were slice time-corrected, motion-corrected to the median image using b-spline interpolation (4 df), high-pass filtered (100 s), and spatially smoothed (8 mm full width at half maximum (FWHM), isotropic). The median functional and anatomical volumes were coregistered, then transformed into the standard anatomical space (T_1 MNI template) using the tri-linear interpolation [Ashburner and Friston, [1999]].

Subject-level statistical analyses used the GLM as implemented in SPM2. The four-condition events were modeled using a canonical hemodynamic response function and maps of the following linear contrasts were produced: (1) truth minus baseline, (2) lie minus baseline, (3) truth minus recurrent distracter, lie minus recurrent distracter, lie minus truth, truth minus lie, and recurrent distracter minus variant distracter. Only voxels significantly activated for the truth minus baseline and lie minus baseline contrasts were retained for further analyses. To control for the potential motor contribution [Langleben et al., [2002]] to the main contrasts, participants were randomly assigned dominant or nondominant response hand. Differences between dominant and nondominant groups were tested with a whole-brain mixed model ANOVA. A similar analysis examined group differences between participants who reported use of any strategy during the task and those that did not (Strategy, No Strategy). For the complete sample group-level random effects analyses were accomplished by entering whole-brain contrasts into one-sample t-tests and resulting SPM {T} maps were transformed to unit normal distribution SPM {Z} maps. Significance thresholds were based on spatial extent using a height of $z \geq 2.57$ and cluster probability $P \leq 0.05$ [Forman et al., [1995]]. This resulted in a corrected probability of $P \leq 0.05$, based on the theory of Gaussian fields [Friston et al., [1993], [1994]]. Identified clusters were then divided into anatomical regions using the Talairach Daemon database [Lancaster et al., [1997]]. For discussion purposes, the Lie - Truth contrast was presented at $P > 0.05$, uncorrected.

Predictive ability at the within-subject, single-event level was evaluated using a stepwise model-building process for logistic regression, with classification and regression trees (CART) used to evaluate potential interactions for the model. Functional regions of interest (ROIs) were derived from the group analysis and applied to a secondary single event regression. Because a group cluster peak may not accurately capture individual activation, we included neighboring voxels (two voxels in 3-D) effectively smoothing percent signal change around the maxima. A total of 19, 125-voxel ROIs (20 × 20 × 20 mm cube) were grown from the cluster maxima of the following initial group contrasts: lie minus recurrent distracter, truth minus recurrent distracter, truth minus lie, and lie minus truth. The mean percent signal change for each ROI was estimated with a second regression model for 48 separate lie and truth events and these data subjected to further analysis.

The area under the curve (AUC) of the receiver operator characteristic (ROC) function, a plot of "1-specificity" (probability of the model wrongly predicting a lie) vs. "sensitivity" (probability of the model correctly predicting a lie) was used to evaluate predictive ability. The AUC is the probability of accurately classifying a pair of observations, where one is truth and one is lie. Secondary measures assessed the percent of observations correctly classified and the odds ratio for truth for each ROI relative to the regional activations.

The AUC was obtained using Logistic Regression Analysis implemented in STATA 8 (Stata, College Station, TX, 2004), with truth vs. lie as the binary outcome and the selected ROIs (mean percent signal change) as the predictor variables. A stepwise approach to selecting the predictor variables was used. ROIs were added as predictors based on improvement in model predictive ability, with the best single predictor added first and additional predictors based on increased predictive ability conditional on the ROIs already included in the model. Predictors could potentially be removed, if in the presence of other predictors they no longer add significant predictive ability (P-value to enter < 0.20, P-value to remove > 0.25). CART analyses [Breiman et al., [1984]; Clark and Pregibon, [1993]] (SPLUS, Mathsoft, Cambridge, MA, 1999) were used to detect potential interactions among ROIs, with these interactions then tested as potential predictors in the stepwise logistic regression models. In order to adjust for multiple

nonindependent observations from each subject (truth/lie outcome for each card presented to each subject), a robust variance correction was used in all logistic regression models [Williams, [2000]].

Validation of the model was addressed with three additional analyses. First, a validation dataset consisting of four additional subjects was assessed. Second, a bootstrap approach was used to assess the reproducibility of the automated stepwise logistic regression model [Styerberg, [2001]], which is more efficient than a split-sample approach. Ten thousand bootstrap samples were selected and the percentage of times each predictor considered was included in the stepwise model was determined. Third, adjustments for "optimism" [Efron and Tibshirani, [1993]] were determined for the prediction error, AUC, and the accuracy of the final stepwise model. Considering the predictors in the final stepwise model, coefficients were determined for each of the 10,000 bootstrap samples. "Optimism" of the prediction error is the excess prediction error that is added to adjust for the fact that the prediction is typically not as good for other datasets. The "optimism" adjustment for the prediction error is the difference between the prediction error from the bootstrap sample and the prediction error from the original data. The "optimism" is added to the prediction error from the final model to obtain an "optimism" adjusted prediction error. Similar adjustments were made for the AUC and the accuracy, where these were both lowered to account for the "optimism."

RESULTS
Behavioral
A significant difference in accuracy ($F_{(3,19)}$ = 9.62, $P < 0.05$) and response time ($F_{(3,19)}$ = 31.44, $P < 0.05$) was observed among the four stimuli classes (Table I). Eleven participants reported intentionally focusing attention on the truth stimuli during the task and 11 participants denied using any strategy.

There was no difference between the "strategy" and "no strategy" cohorts in the performance accuracy ($F_{(1,20)}$ = 0.24, $P = 0.63$) or speed ($F_{(1,20)}$ = 1.84, $P = 0.19$). All subjects were right-handed. When comparing participants responding with dominant (right) vs. nondominant (left) hand, again there was no difference between groups for accuracy ($F_{(1,20)}$ = 0.13, $P = 0.72$) or speed ($F_{(1,20)}$ = 0.03, $P = 0.86$).

fMRI Group Results
When Lie was contrasted with Repeat Distracter (nonsalient truth), significant cluster centroids were located in left inferior frontal gyrus (IFG), Brodmann area (BA) 13, right IFG (BA 47), right medial frontal gyrus (MFG) (BA 8), and right supramarginal gyrus (BA 40) (Figure 1, Table II). Subregions within right MFG cluster included superior and medial frontal gyri bilaterally (BA 8, 9) extending to the right supplementary motor area (SMA, BA 6) and the ACC (BA 32). The IFG (BA 47) cluster included BA 44, 45, and 46, the lateral aspect (frontal eye field, FEF) of the precentral gyrus (BA 6), and the insula (BA 13). Finally, the right inferior parietal lobule (IPL) and the adjacent superior temporal gyrus (BA 22) showed activation within the supramarginal gyrus (BA 40) cluster.
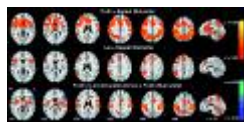
Figure 1. Group analysis (n = 22) showing significant differences in brain activation between Lie, Truth, and Repeat Distracter conditions. Row 1: Truth > Repeat Distracter; row 2: Lie > Repeat Distracter; row 3: Lie > Truth (blue scale) Truth > Lie (red scale). Images are displayed over a Talairach-normalized template in radiological convention. Significance thresholds for all contrasts based on spatial extent using a height of z ≥ 2.57 and cluster probability $P \leq 0.05$, except Lie > Truth (blue scale) presented at a z ≥ 1.64, uncorrected. See Tables 2-4 for anatomical localization. [Normal View 75K | Magnified View 246K]

Table II. Mean cluster location and local maxima of BOLD signal change for Lie > Repeat Distracter

Cluster number	Size (voxels)	Cerebral hemisphere	Region (Brodmann area)	P (nmax ≥ k)	Z score	x, y, z

1	**427**	R	Inferior frontal gyrus (47)	<0.0001		34, 22, -8
	188	R	Inferior frontal gyrus (13, 44, 45, 47)		4.40	37, 19, -11
	147	R	Middle frontal gyrus (6,8,9,46)		4.25	56, 26, 17
	29	R	Precentral gyrus (6,44)		4.22	56, 12, 3
	17	R	Insula (13)		3.51	37, 19, -1
	10	R	Superior temporal gyrus (38)		3.72	51, 15, -14
2	**241**	R	Medial frontal gyrus (8)	0.001		8, 34, 40
	72	R	Medial frontal gyrus (6,8,9)		5.45	12, 31, 35
	64	R	Superior frontal gyrus (8)		4.79	16, 18, 51
	10	R	Cingulate gyrus (32)		3.64	7, 21, 36
3	**191**	R	Supramarginal gyrus (40)	0.002		56, -52, 36
	126	R	Inferior parietal lobule (40)		4.49	48, -48, 50
	44	R	Supramarginal gyrus (40)		4.54	59, -45, 32
	8	R	Superior temporal gyrus (22)		3.36	56, -50, 17
	3	R	Superior parietal lobule (7)		3.30	42, -60, 47
4	**105**	L	Inferior frontal gyrus (13)	0.016		-30, 14, -14
	57	L	Inferior frontal gyrus (13,45,47)		4.44	-26, 11, -17
	9	L	Precentral gyrus (6)		4.27	-38, 16, 3
	23	L	Insula (13)		3.83	-34, 16, 3

Cluster height threshold z ≥2.57; probability threshold < 0.05.
Estimated Brodmann's areas and coordinates from Talairach and Tournoux [[1988]].
Z values represent peak activation for atlas-derived subdivisions greater than two voxels.

Table III. Mean cluster location and local maxima of BOLD signal change for Truth > Lie

Cluster number	Size (voxels)	Cerebral hemisphere	Region (Brodmann area)	P (nmax $\geq$ k)	Z score	x, y, z
1	**1,475**	L	Inferior parietal lobule (40)	<0.0001		-42, -32, 42
	97	L	Inferior parietal lobule (40)		6.21	-37, -34, 39
	116	L	Postcentral gyrus (1,2,3,5,40)		5.74	-37, -34, 46
	51	L	Middle frontal gyrus (6)		5.08	-24, -13, 52
	61	L	Precentral gyrus (4,6)		4.98	-26, -13, 52
	21	L	Superior frontal gyrus (?)		4.91	-26, -12, 63
	47	L	Medial frontal gyrus (6)		4.20	-12, -13, 49
	31	L	Cingulate gyrus (24)		4.12	-4, -2, 30
	26	L	Superior parietal lobule (7)		4.03	-24, -52, 58
	43	L	Precuneus (7)		3.95	-12, -50, 54
	22	L	Anterior cingulate (32)		3.54	-12, 20, 21
	26	R	Precentral gyrus (4)		5.24	63, -22, 31
	239	R	Postcentral gyrus (1,2,3,5,7,40)		5.05	63, -22, 27
	95	R	Inferior parietal lobule (40)		4.48	63, -24, 23
	41	R	Superior parietal lobule (7)		4.24	30, -50, 58
	85	R	Precuneus (7)		4.03	24, -50, 54
	13	R	Medial frontal gyrus (6)		3.79	4, -2, 44
	18	R	Cingulate gyrus (24)		3.71	4, -2, 41
2	**651**	R	Cerebellum	<0.0001		4, -60, -18
	178	R	Declive		4.74	7, -63, -20
	145	R	Culmen		4.45	7, -59, -21
	95	L	Culmen		4.31	-15, -52, -24
	37	L	Cerebellar tonsil		4.05	-22, -49, -35
3	**206**	L	Inferior frontal gyrus (9)	<0.0001		-56, 6, 26
	16	L	Inferior frontal gyrus (9,44)		4.52	-53, 1, 22

			Region (Brodmann area)	P (uncorr.)	Z score	x, y, z
	23	L	Precentral gyrus (6,44)		4.48	-53, -3, 22
	32	L	Putamen		4.37	-26, -7, 8
	32	L	Insula (13)		4.27	-30, -7, 8
	91	L	Thalamus		4.20	-12, -25, 12
4	**123**	R	Superior frontal gyrus (6)	<0.0001		26, -4, 66
	25	R	Superior frontal gyrus (6)		5.38	30, -8, 63
	38	R	Middle frontal gyrus (6)		5.03	30, -13, 56
	40	R	Precentral gyrus (4)		4.83	37, -17, 52
5	**100**		Right inferior frontal gyrus (9)	<0.0001		60, 10, 26
	24	R	Inferior frontal gyrus (9,44)		4.69	63, 5, 22
	29	R	Insula (13)		4.47	42, -7, 8
	12	R	Precentral gyrus (6,44)		4.06	63, 1, 22
	12	R	Lentiform nucleus		3.93	34, -8, 4
	23	R	Claustrum		3.67	38, -11, 8

Cluster height threshold $Z \geq 2.57$; probability threshold < 0.05.
Estimated Brodmann's areas and coordinates from Talairach and Tournoux [[1988]].
Z values represent peak activation for atlas-derived subdivisions greater than two voxels.

Table IV. Location of local maxima of BOLD signal change for Lie > Truth

Cerebral hemisphere	Region (Brodmann area)	P (uncorr.)	Z score	x, y, z
L	Inferior frontal gyrus (45)	0.0038	2.67	-50, 20, 14
L	Superior frontal gyrus (8)	0.0039	2.66	-4, 34, 44
L	Superior frontal gyrus (8)	0.0073	2.44	-38, 12, 48
L	Middle frontal gyrus (47)	0.0192	2.07	-38, 34, -12

Uncorrected threshold $Z \geq 1.64$; minimum of 8 voxels.
Estimated Brodmann's areas and coordinates from Talairach and Tournoux [[1988]].
Z values represent peak activation for uncorrected cluster.

At this threshold, the Lie minus Truth contrast (Figure 1, Table III) yielded no significant clusters. When examined at a threshold of $P \geq 0.05$ uncorrected, peak Z scores were located within regions significant in the Lie minus Repeat Distracter contrast. These included the left IFG (BA 44-47), the medial left SFG and MFG, and medial frontal cortex (BA 6, 8).

Several regions showed greater activation to the salient Truth condition than to the Lie trials (Figure 1, Table IV). Significant clusters were seen in IPL bilaterally (BA 40), extending to the postcentral gyrus, the superior parietal lobule (SPL), BA 1-5, 7, and the precuneus (BA 7). Activation was also seen in the lateral aspect of the left MFG and precentral frontal gyri (FEF, BA 4,6), medial aspect (SMA) of the right MFG (BA 6), the cingulate gyrus (BA 24), and the left ACC (BA 32), the bilateral cerebellum: tonsils, pyramis, and uvulae, and the bilateral IFG (BA 9) extending to the precentral cortex (6, 44), striatum, insula, and the left thalamus.

A group main effect (dominant vs. nondominant) was seen in the primary motor cortices with circumscribed activation for right-hand responders located in the left precentral gyrus (BA 4) and for the left-hand responders in the right precentral gyrus (BA 4). When comparing dominant and nondominant response hand groups for contrasts between stimuli classes requiring a button press (e.g., Lie > Repeat, Truth > Repeat, Lie > Truth, Truth > Lie), no regions showed a main effect. Analyses examining group differences between participants who reported intentionally focusing on the "truth" target and those who were not aware of using a strategy showed no group main effect.

Logistic Regression Analysis of Within-Subject Single-Event fMRI Data

Average percent signal change in 19 significant ROIs (Table V) for the Lie or Truth conditions (from multisubject average presented in Fig. 1), were tested for their ability to accurately classify Lie and Truth trials. First, each ROI was assessed for predictive ability of truth vs. lie using a logistic regression (adjusting parameter variances for nonindependent observations). The best single predictor was the left IPL (BA 40). AUC for this ROI alone was 0.7509, with an accuracy of 67.27% (percent correctly classified), and an odds ratio (OR) of 0.6401. The next-best single predicting ROI was left MFG (BA 6), with an AUC of 0.7160, an accuracy of 74.36%, and an OR of 0.6788. The third-best ROI was left IFG (BA 45), AUC = 0.6496, an accuracy of 62.73%, OR = 1.2. Stepwise logistic regression was then used to construct a model containing the set of regions that can best predict lie vs. truth. Potential interactions of the selected regions were assessed using CART, with these interactions then tested for inclusion in the final logistic regression model. The tree from CART (Fig. 2) shows that the first four most predictive potential interactions are ROIs 1, 2, 9, and 14. None of the interactions with ROI 9 were significant in the logistic regression model and so were excluded from further analysis. Two- and three-way interactions of 1, 2, and 14 (left IFG, MFG, and IPL) were considered for inclusion in the final model.

Table V. ROIs identified by logistic regression and the predictive ability of individual ROI activations, based on a separate logistic regression model for each ROI

ROI	Region (Brodmann area)	AUC	Accuracy	OR	OR (P)	95% CI, lower limit OR	95% CI, upper limit OR
1	Left inferior frontal gyrus (45)	0.6496	62.73	1.1949	<0.001	1.1158	1.2797
2	Left inferior parietal lobule (40)	0.7509	67.27	0.6401	<0.001	0.5797	0.7069
3	Right middle temporal gyrus (37)	0.6428	60.64	0.7980	<0.001	0.7142	0.8916
4	Right cuneus (18)	0.6512	62.27	0.8381	<0.001	0.7812	0.8992
5	Right medial frontal gyrus (8)	0.5705	56.82	1.0561	0.020	1.0085	1.1059
6	Right supramarginal gyrus (40)	0.5456	53.82	1.0432	0.061	0.9980	1.0905
7	Left inferior frontal gyrus (13)	0.5646	55.09	1.0540	0.040	1.0023	1.1083
8	Right inferior frontal gyrus (47)	0.5671	55.09	1.0619	0.049	1.0003	1.1273
9	Left inferior parietal	0.5328	52.91	1.0224	0.277	0.9824	1.0641

	lobe (40)					
10	Right middle temporal gyrus	0.5355	53.45	1.0406 0.078	0.9955	1.0878
11	Left middle frontal gyrus (8)	0.5737	55.73	1.0536 0.061	0.9975	1.1128
12	Right precuneus (7)	0.4909	52.00	0.9982 0.909	0.9677	1.0296
13	Left inferior parietal lobule (40)	0.7156	65.18	0.6854 <0.001	0.6203	0.7573
14	Left middle frontal gyrus (6)	0.7160	64.36	0.6788 <0.001	0.6158	0.7481
15	Right fusiform gyrus (37)	0.6200	59.00	0.8654 0.018	0.7679	0.9752
16	Right middle frontal gyrus (11)	0.5782	57.00	0.9079 <0.001	0.8650	0.9528
17	Right middle temporal gyrus (37)	0.5967	57.27	0.8847 <0.001	0.8382	0.9337
18	Left cerebellum	0.6174	58.64	0.8777 <0.001	0.8192	0.9403
19	Left cingulate gyrus (23)	0.5514	53.55	0.9037 <0.001	0.8557	0.9544

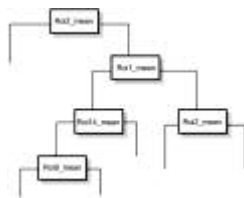ROI, Region of interest; AUC, area under curve; OR, odds ratio; CI, confidence interval.

Figure 2. Classification and regression trees (CART) plot, showing the first six nodes (up to three-way interactions) for the peak and mean MRI signal (max and min). All 19 brain regions were included in the full tree applied to the single trials data.
[Normal View 12K | Magnified View 29K]

The final stepwise logistic regression model, allowing potential inclusion of each ROI and of the interaction terms for all included regions, is shown in Table VI. The final model includes 14 ROIs, as well as three two-way interactions and one three-way interaction. The final model has an AUC of 0.8467. The prediction error, which is the mean squared error of the predicted probability of the outcome being a lie, was 0.1593. Using this model for prediction of the observed experiment, it correctly classifies 78.00% of the observations with a sensitivity of 76.33% and specificity of 79.55% (Fig. 3). The positive predictive value (PPV) was 0.7750 and the negative predictive value (NPV) was 0.7845. Ignoring the interactions detected by CART, the AUC was reduced from 84.67 to 84.38% and percent correct was reduced to 77.18%.

Table VI. Final logistic regression model results

ROI	OR	SE	Z-Score	P	95% CI, lower limit	95% CI, upper limit	Bootstrap stepwise models, including predictor (%)
ROI 1	1.2685	0.061608	4.90	<0.001	1.1533	1.3952	99.99
ROI 2	0.7576	0.062549	-3.36	0.001	0.6443	0.8906	99.82
ROI 3	0.8947	0.061359	-1.62	0.105	0.7821	1.0233	87.32
ROI 4	0.9192	0.039204	-1.98	0.048	0.8454	0.9993	94.35
ROI 6	1.0747	0.037587	2.06	0.039	1.0035	1.1509	72.26
ROI 8	1.1695	0.046913	3.90	<0.001	1.0810	1.2651	99.90
ROI 10	1.0970	0.039449	2.58	0.010	1.0223	1.1771	82.67

ROI 11	1.0883	0.033178	2.77	0.006	1.0251	1.1552	92.70
ROI 12	1.1080	0.030318	3.75	<0.001	1.0501	1.1690	99.27
ROI 13	1.1630	0.068411	2.57	0.010	1.0363	1.3050	48.67
ROI 14	0.6906	0.043537	-5.87	<0.001	0.6103	0.7814	95.56
ROI 16	0.9175	0.036627	-2.16	0.031	0.8484	0.9922	88.30
ROI 17	0.8522	0.042008	-3.24	0.001	0.7737	0.9386	99.51
ROI 18	0.9255	0.033836	-2.12	0.034	0.8614	0.9942	88.62
ROI 1 × ROI 2	0.9838	0.023633	-0.68	0.496	0.9385	1.0311	87.60
ROI 1 × ROI 14	1.0281	0.013920	2.05	0.041	1.0011	1.0557	
ROI 2 × ROI 14	0.9990	0.014960	-0.04	0.972	0.9705	1.0292	
ROI 1 × ROI 2 × ROI 14	0.9914	0.002312	-3.71	<0.001	0.9868	0.9959	

Percentage of bootstrap stepwise models including predictors not in final model; 0% for ROI 5, 7, 9, 19, and 26.70% for ROI 15.

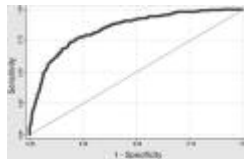ROI, region of interest; OR, odds ratio; SE, standard error; CI, confidence interval.

Figure 3. GKT2 receiver operator characteristic curve (ROC) of the final logistic regression model for the group analysis corresponds to the logistic regression model that includes all terms from the CART model, up to three-way interactions. The AUC (e.g., the accuracy of prediction) is 0.8467 (chance = 0.5).
[Normal View 21K | Magnified View 43K]

The final model (shown in Table VII) was validated using three approaches. First, the predictive ability of the model was determined for four additional participants, demographically matched to the main cohort, serving as a validation sample. Using the same paradigm as above, the final logistic regression model predicted lie vs. truth for these four participants with an accuracy of 76.5% (153/200), sensitivity of 68.8% (66/96), specificity of 83.7% (87/104), PPV of 79.5% (66/83), and NPV of 74.4% (87/117). This validates the model's high predictive ability. Second, for 10,000 bootstrap samples the percentage of times each predictor considered was included in the stepwise model was determined (right column, Table VI). All predictors in the final model were included in a large percentage of the bootstrap models. Furthermore, predictors not included in the final model were included in small percentages of the bootstrap models or not included at all (note that the three-way interaction was highly significant and therefore the three-way and two-way interactions were included or excluded as a group). This validates the choice of the predictors included in the final stepwise model. Third, the "optimism" adjusted values of predictive ability were determined. These were: a prediction error of 0.1658 (an increase of 0.0064 for "optimism"), an AUC of 83.62% (a decrease of 1.05 for "optimism"), and an accuracy of 77.12% (a decrease of 0.88 for "optimism"). Thus, there are only very small changes in the measures assessing predictive ability after adjustment for "optimism," which adjusts for the expected differences that would be observed if the final model were fit to additional subjects.

DISCUSSION

The results indicate that the attentional orientation system involved in the visual target and novelty processing, and the working memory system involved in contextual processing, are active during deceptive behavior. Though partially overlapping, the attentional system involves parietal and insular cortex and subcortical nuclei, while the contextual system usually includes the medial and lateral prefrontal cortex (BA 6, 8, 9, and 44-47). ACC activation has been reported in both, although there may be anteroposterior segregation between the BA 32 and 24 components [Bush et al., [1999]]. As hypothesized, when compared to a control (truth) condition of lower relative salience, lie trials activated both the attentional and the contextual working memory system. Consistent with earlier studies [Spence et al., [2004]], this included the bilateral inferior lateral and superior medial frontal cortices (including the ACC), the lateral and medial premotor cortex (SMA and FEF), the right inferior parietal cortex, and the insulae (Fig. 2). In the salience-controlled contrast, however, Lie-related activation was both less robust

and limited to areas associated with context processing - the left IFG (BA 44-47) and the medial (SMA) and lateral (FEF) aspects of the left SFG (BA 6 and 8). Activation in the Truth vs. Lie contrast was closer to the attentional circuitry, since in addition to the rostral left ACC (BA 32), the medial and lateral prefrontal gyri, and the IPL (BA 40) of the inferior parietal cortex, it also involved the dorsal part of the ACC (BA 24), the precuneus, the SPL (BA 7, 5), and the left thalamus. All these were seen in addition to the parietal (BA 40) activation, which is also found in the nonsalience controlled Lie contrast. In each frontal cortical region where Truth and Lie related activation partially overlapped, Truth-related activation was posterior to Lie. This pattern is consistent with the hypothesis of the anteroposterior hierarchical organization of the prefrontal cortex and supports the notion that Truth responses required less working memory effort than Lie [Koechlin et al., [2003]; Pochon et al., [2002]].

Together with the behavioral results and the task structure, the activation pattern of Lie and Truth suggests that they are mediated by similar networks. Truth was associated with the longest RT, followed by Lie, while the only strategy consistently employed by participants was to "ignore" the Lie item and focus on the Truth item. These findings indicate that the direction of the differences between lie and truth was influenced by the relative salience of the lie and truth items and is thus task-dependent. These data also allow inference about the basic neural components of deception, at least within a forced-choice paradigm; the inferior lateral prefrontal (BA 44-47) and medial superior frontal (BA 9) cortices were activated in both salience-controlled and nonsalience-controlled Lie contrasts, indicating potential specificity for lie.

The significance of inferior lateral prefrontal and medial superior frontal regions to deception is confirmed by results of the logistic regression analysis, since the left inferior lateral cortex was among the four regions that contributed most to the Lie/Truth discrimination: the left IFG, the parietal somatosensory IPL (BA 40), and the premotor (BA6) and the MFG (BA8). Inferolateral PFC had the highest OR for Lie, indicating a positive association with deception. Since the ACC was not among these regions, it is less likely to be predictive of Lie. Remarkably, the somatosensory association area (BA 40) and the insulae have been associated with the electrodermal response [Critchley et al., [2000]; Tranel and Damasio, [1994]]. In our experiment the insulae were activated in both Lie and Truth contrasts, but the activation in the Lie-Repeat contrast was anterior to the Truth-Lie contrast. The anterior insula is central in the mediation and integration of the afferent interoceptive (somatic) input, and thus could link the deception-related brain activity with the peripheral indices of arousal used in the physiological lie-detection with the "polygraph" [Critchley et al., [2004]; Tranel and Damasio, [1994]]. The somatosensory association area was activated by the nonsalience controlled Lie and in Truth contrasts and could therefore be driven by salience, deception, or both. Indeed, an efficient task performance involved assigning greater attention to the Truth item as the item to be "sacrificed" and attempting to ignore the Lie item, further reducing the salience of the Lie relative to the Repeat Distracter. This approach has been used as a successful countermeasure to a similar task in an EEG study [Rosenfeld, [2004]].

The left inferior and middle frontal cortex has been implicated in response inhibition [Konishi et al., [2003]; Rubia et al., [2003]; Schulz et al., [2004]] and memory suppression [Anderson et al., [2004]]; however, the functions of this area extend beyond response inhibition. Joint activation of the inferolateral frontal cortex (BA 44-47) and the SMA (BA 6) has been associated with generation of language and other speech (e.g., sign-language) [Horwitz et al., [2003]] and response selection in paradigms requiring task switching or outcome assessment [Lau et al., [2004]; Paulus et al., [2004]; Rowe et al., [2000]; Turk et al., [2004]; Zhang et al., [2004]]. Activation in the BA 44-45, BA 40, bilateral dorsal and left medial BA 6, left ACC, and BA 8 was also correlated with increasing working memory load [Nunez et al., [2005]; Zarahn et al., 2004]. The lateral and medial premotor, the anterior cingulate, and the associative somatosensory parietal cortices are the areas that have been activated in deception paradigms in which the lie item was more salient than truth [Langleben et al., [2002]; Spence et al., [2001]]. Together with the behavioral results, these data indicate that in the GKT2, salience of the Truth condition matched or surpassed the Lie.

Our data indicate that the left inferior frontal and somatosensory associative medial premotor areas form a network involved in generating deceptive responses under the conditions of a forced-choice model of deception. The fact that Truth-related activation was more robust than Lie contradicts the assumption that truth is invariably a "default" routine response [Langleben et al., [2002]; Spence et al., [2004]]. Nevertheless, the data still support the concept of deception as a relatively more complex cognitive function than truth-telling because of the rostral location of the lie-related activation, and given the role of the left inferior frontal and medial premotor activation in response selection and inhibition. The association between deception and inhibition could explain why involuntary discharge of information that has been

described as "Freudian slip" is more common during increased cognitive load or reduced inhibitory control [Schulz et al., [2004]]. Thus, the final common denominator of intentional deception could be conceptualized as a conscious act of suppression of information that is subjectively true. This may or may not be accompanied by a release of subjectively false information. Remarkably, this definition resonates closely with the Augustinian: "deception is denying what is" definition [Augustine, [1948]]. If the ultimate goal of detecting a lie is collecting information about what an individual knows, fMRI can be beneficial in conjunction with activation paradigms aimed at brain correlates of semantic memory [Hirsch et al., [2001]; Mecklinger et al., [2000]; Nystrom et al., [2000]]. While a potential confound in characterization of the neural mechanisms of deception, in such case salience could serve as a marker of concealed or unconscious knowledge [Berns et al., [1997]; Tranel and Damasio, [1985]].

The logistic regression analysis confirmed our second hypothesis on the feasibility of using fMRI for the detection of lie events in an individual. The combined AUC of all the mean values for ROIs identified by the group analysis in the Lie-Truth and Truth-Lie contrasts yielded a moderately high accuracy of 78% for the classification of individual events as Lie or Truth. The fMRI-GKT2 combination appears to be more specific than sensitive, suggesting a potential as a confirmatory test rather than a screening device. Adjustments for "optimism" that included bootstraps of the logistic regression indicated that very similar performance estimates would be obtained in replication. These results are the first reported formal quantification of the accuracy of fMRI-based methods for the detection of deception at the within-subject, single-event level.

Although fMRI-based Lie-Truth discrimination was possible even after controlling for the effects of salience, the effect size of Lie was reduced by matching or overmatching the salience of the Truth condition. This indicates that the accuracy achieved here is a low estimate of the potential accuracy of lie-detection with fMRI. The scenario of GKT2 was of low ecological relevance and risk. A task of higher ecological relevance and risk may induce larger effects and have higher accuracy. Another limitation of the GKT2 design is the lack of free choice to lie or tell the truth on specific items. This was partially offset by allowing participants to choose the Lie item. Modeling questions and answers separately, which is beyond our current capability, may permit better discrimination of item salience from response salience. Our study examined healthy participants, and may not generalize to abnormal populations [Vollm et al., [2004]]. Future studies could examine the effects of cognitive and pharmacological countermeasures and physiological states on the accuracy of fMRI-based lie detection.

CONCLUSIONS

In the setting of a forced choice paradigm, some of the brain activity previously attributed to deception has been driven by the task design, in particular by the relative attentional value of the comparison items. Although lie and truth are mediated by a similar frontoparietal network, lie appears to be a more working memory-intensive activity, characterized by increased activation of the inferolateral cortex implicated in response selection, inhibition, and generation. Accurate classification of single Lie and Truth events is possible within the reported forced choice model and may improve further in an ecologically relevant scenario within similar task structure. The high classification accuracy achieved under the present task confirms the feasibility of a practical fMRI based lie-detection system.

REFERENCES

Anderson MC, Ochsner KN, Kuhl B, Cooper J, Robertson E, Gabrieli SW, Glover GH, Gabrieli JD (2004): Neural systems underlying the suppression of unwanted memories. *Science* **303**: 232-235.

Ashburner J, Friston KJ (1999): Nonlinear spatial normalization using basis functions. *Hum Brain Mapp* **7**: 254-266.

Augustine St (1948): "De mendacio." In: *Opuscules. II. Problèmes moraux.* Paris: Desclée de Brouwer et Cie. p 244-245.

Bandettini PA, Wong EC, Hinks RS, Tikofsky RS, Hyde JS (1992): Time course EPI of human brain function during task activation. *Magn Reson Med* **25**: 390-397.

Berns GS, Cohen JD, Mintun MA (1997): Brain regions responsive to novelty in the absence of awareness. *Science* **276**: 1272-1275.

Breiman L, Friedman JH, Olshen RA, Stone CJ (1984): *Classification or regression trees*. Belmont, CA: Wadsworth International Group.

Bush G, Frazier JA, Rauch SL, Seidman LJ, Whalen PJ, Jenike MA, Rosen BR, Biederman J (1999): Anterior cingulate cortex dysfunction in attention-deficit/hyperactivity disorder revealed by fMRI and the Counting Stroop. *Biol Psychiatry* **45**: 1542-1552.

Cabeza R, Dolcos F, Prince SE, Rice HJ, Weissman DH, Nyberg L (2003): Attention-related activity during episodic memory retrieval: a cross-function fMRI study. *Neuropsychologia* **41**: 390-399.

Chute DL, Westall RF (1997): *PowerLaboratory*. Devon, PA: MacLaboratory.

Clark LA, Pregibon D (1993): Tree-based models. In: Chambers JM , Hastie TJ , editors. *Statistical models*. New York: Chapman & Hall. p 377-419.

Cohen JD (1988): *Statistical power analysis for the behavioral sciences*, 2nd ed. Hillsdale, NJ: Lawrence Erlbaum.

Critchley HD, Elliott R, Mathias CJ, Dolan RJ (2000): Neural activity relating to generation and representation of galvanic skin conductance responses: a functional magnetic resonance imaging study. *J Neurosci* **20**: 3033-3040.

Critchley HD, Wiens S, Rotshtein P, Ohman A, Dolan RJ (2004): Neural systems supporting interoceptive awareness. *Nat Neurosci* **7**: 189-195.

Efron B, Tibshirani RJ (1993): *An introduction to the bootstrap*. London: Chapman & Hall.

Ekman P (2001): *Telling lies*. New York: Norton.

Forman SD, Cohen JD, Fitzgerald M, Eddy WF, Mintun MA, Noll DC (1995): Improved assessment of significant activation in functional magnetic resonance imaging (fMRI): use of a cluster-size threshold. *Magn Reson Med* **33**: 636-647.

Friston KJ, Worsley KJ, Frackowiak RSJ, Mazziotta JC, Evans AC (1993): Assessing the significance of focal activations using their spatial extent. *Hum Brain Mapp* **1**: 210-220.

Friston KJ, Jezzard P, Turner R (1994): Analysis of functional MRI time-series. *Hum Brain Mapp* **1**: 153-171.

Ganis G, Kosslyn SM, Stose S, Thompson WL, Yurgelun-Todd DA (2003): Neural correlates of different types of deception: an fMRI investigation. *Cereb Cortex* **13**: 830-836.

Gur R, Sackeim HA (1979): Self-deception: a concept in search of a phenomenon. *J Pers Soc Psychol* **37**: 147-169.

Gur RC, Turetsky BI, Loughead J, Waxman J, Snyder WE, Ragland JD, Elliott M, Bilker WM, Arnold SE, Gur RE (2004): Detection of visual target and novel stimuli demonstrated with event-related fMRI. In: Society for Neuroscience, Program No. 480.485. San Diego: Society for Neuroscience.

Hester R, Fassbender C, Garavan H (2004): Individual differences in error processing: a review and reanalysis of three event-related fMRI studies using the GO/NOGO task. *Cereb Cortex* **14**: 986-994.

Hirsch J, Moreno DR, Kim KH (2001): Interconnected large-scale systems for three fundamental cognitive tasks revealed by functional MRI. *J Cogn Neurosci* **13**: 389-405.

Horwitz B, Amunts K, Bhattacharyya R, Patkin D, Jeffries K, Zilles K, Braun AR (2003): Activation of Broca's area during the production of spoken and signed language: a combined cytoarchitectonic mapping and PET analysis. *Neuropsychologia* **41**: 1868-1876.

Huettel SA, McCarthy G (2004): What is odd in the oddball task? Prefrontal cortex is activated by dynamic changes in response strategy. *Neuropsychologia* **42**: 379-386.

Koechlin E, Ody C, Kouneiher F (2003): The architecture of cognitive control in the human prefrontal cortex. *Science* **302**: 1181-1185.

Konishi S, Jimura K, Asari T, Miyashita Y (2003): Transient activation of superior prefrontal cortex during inhibition of cognitive set. *J Neurosci* **23**: 7776-7782.

Kozel FA, Padgett TM, George MS (2004): A replication study of the neural correlates of deception. *Behav Neurosci* **118**: 852-856.

Lancaster JL, Rainey LH, Summerlin JL, Freitas CS, Fox PT, Evans AC, Toga AW, Mazziotta JC (1997): Automated labeling of the human brain: a preliminary report on the development and evaluation of a forward-transform method. *Hum Brain Mapp* **5**: 238-242.

Langleben DD, Schroeder L, Maldjian JA, Gur RC, McDonald S, Ragland JD, O'Brien CP, Childress AR (2002): Brain activity during simulated deception: an event-related functional magnetic resonance study. *Neuroimage* **15**: 727-732.

Langleben DD, Loughead JW, Bilker W, Phend N, Busch S, Childress AR, Platek SM, Wolf R, Gur RC (2004): *Imaging deception with fMRI: the effects of salience and ecological relevance*. Program No. 372.312. Abstract Viewer/Itinerary Planner, www.sfn.org, online. San Diego: Society for Neuroscience.

Lau HC, Rogers RD, Ramnani N, Passingham RE (2004): Willed action and attention to the selection of action.

Neuroimage **21**: 1407-1415.

Lee TM, Liu HL, Tan LH, Chan CC, Mahankali S, Feng CM, Hou J, Fox PT, Gao JH (2002): Lie detection by functional magnetic resonance imaging. *Hum Brain Mapp* **15**: 157-164.

Mecklinger A, Bosch V, Gruenewald C, Bentin S, von Cramon DY (2000): What have Klingon letters and faces in common? An fMRI study on content-specific working memory systems. *Hum Brain Mapp* **11**: 146-161.

Nunez JM, Casey BJ, Egner T, Hare T, Hirsch J (2005): Intentional false responding shares neural substrates with response conflict and cognitive control. *Neuroimage* **25**: 267-277.

Nystrom LE, Braver TS, Sabb FW, Delgado MR, Noll DC, Cohen JD (2000): Working memory for letters, shapes, and locations: fMRI evidence against stimulus-based regional organization in human prefrontal cortex. *Neuroimage* **11**: 424-446.

Paulus MP, Feinstein JS, Tapert SF, Liu TT (2004): Trend detection via temporal difference model predicts inferior prefrontal cortex activation during acquisition of advantageous action selection. *Neuroimage* **21**: 733-743.

Pochon JB, Levy R, Fossati P, Lehericy S, Poline JB, Pillon B, Le Bihan D, Dubois B (2002): The neural system that bridges reward and cognition in humans: an fMRI study. *Proc Natl Acad Sci U S A* **99**: 5669-5674.

Rosenfeld PJ (2004): Simple, effective countermeasures to P-300-based tests of detection of concealed information. *Psychophysiology* **41**: 205-219.

Rosenfeld JP, Cantwell B, Nasman VT, Wojdac V, Ivanov S, Mazzeri L (1988): A modified, event-related potential-based guilty knowledge test. *Int J Neurosci* **42**: 157-161.

Rowe JB, Toni I, Josephs O, Frackowiak RS, Passingham RE (2000): The prefrontal cortex: response selection or maintenance within working memory? *Science* **288**: 1656-1660.

Rubia K, Smith AB, Brammer MJ, Taylor E (2003): Right inferior prefrontal cortex mediates response inhibition while mesial prefrontal cortex is responsible for error detection. *Neuroimage* **20**: 351-358.

Schulz KP, Fan J, Tang CY, Newcorn JH, Buchsbaum MS, Cheung AM, Halperin JM (2004): Response inhibition in adolescents diagnosed with attention deficit hyperactivity disorder during childhood: an event-related fMRI study. *Am J Psychiatry* **161**: 1650-1657.

Spence SA, Farrow TF, Herford AE, Wilkinson ID, Zheng Y, Woodruff PW (2001): Behavioural and functional anatomical correlates of deception in humans. *Neuroreport* **12**: 2849-2853.

Spence SA, Hunter MD, Farrow TF, Green RD, Leung DH, Hughes CJ, Ganesan V (2004): A cognitive neurobiological account of deception: evidence from functional neuroimaging. *Philos Trans R Soc Lond B Biol Sci* **359**: 1755-1762.

Stern PC (2002): *The polygraph and lie detection*. Report of the National Research Council Committee to Review the Scientific Evidence on the Polygraph., 1st ed. Washington, DC: National Academies Press.

Styerberg EW, Harrell FE, Bosboom GJJM, Eijkemans MJC, Vergouwe Y, Habbema JDF (2001): Internal validation of predictive models: efficiency of some procedures for logistic regression analysis. *J Clin Epidemiology* **54**: 774-781.

Talairach J, Tournoux P (1988): *Co-planar stereotaxic atlas of the human brain. 3-Dimensional proportional system: an approach to cerebral imaging*. New York: Thieme Medical.

Tranel D, Damasio AR (1985): Knowledge without awareness: an autonomic index of facial recognition by prosopagnosics. *Science* **228**: 1453-1454.

Tranel D, Damasio H (1994): Neuroanatomical correlates of electrodermal skin conductance responses. *Psychophysiology* **31**: 427-438.

Turk DJ, Banfield JF, Walling BR, Heatherton TF, Grafton ST, Handy TC, Gazzaniga MS, Macrae CN (2004): From facial cue to dinner for two: the neural substrates of personal choice. *Neuroimage* **22**: 1281-1290.

Vollm B, Richardson P, Stirling J, Elliott R, Dolan M, Chaudhry I, Del Ben C, McKie S, Anderson I, Deakin B (2004): Neurobiological substrates of antisocial and borderline personality disorder: preliminary results of a functional fMRI study. *Crim Behav Ment Health* **14**: 39-54.

Vrij, A (2001): *Detecting lies and deceit: the psychology of lying and the implications for professional practice*. Chichester: Wiley; 2001.

Williams RL (2000): A note on robust variance estimation for cluster-correlated data. *Biometrics* **56**: 645-646.

Wolpe PR, Foster KR, Langleben DD (2005): Emerging neurotechnologies for lie-detection: promises and perils. *Am J Bioeth* **5**: 39-49.

Zarahn E, Rakitin B, Abela D, Flynn J, Stern Y (2005): Positive evidence against human hippocampal involvement in working memory maintenance of familiar stimuli. *Cereb Cortex* **15**: 303-316.

Zhang JX, Feng CM, Fox PT, Gao JH, Tan LH (2004): Is left inferior frontal gyrus a general mechanism for

selection? *Neuroimage* **23**: 596-603.